Journal of Materials Chemistry A

Accepted Manuscript

ROYAL SOCIETY OF CHEMISTRY

www.rsc.org/materialsA

15.76% Efficiency Perovskite Solar Cell Prepared under High Relative Humidity: Importance of PbI_2 Morphology in Two-Step Deposition of $CH_3NH_3PbI_3$

Hyun-Seok Ko, Jin-Wook Lee, and Nam-Gyu Park*

School of Chemical Engineering and Department of Energy Science, Sungkyunkwan University, Suwon, 440-746, Korea

*Corresponding author:

N.-G.P.: E-mail address: npark@skku.edu; Tel: +82-31-290-7241

TOC

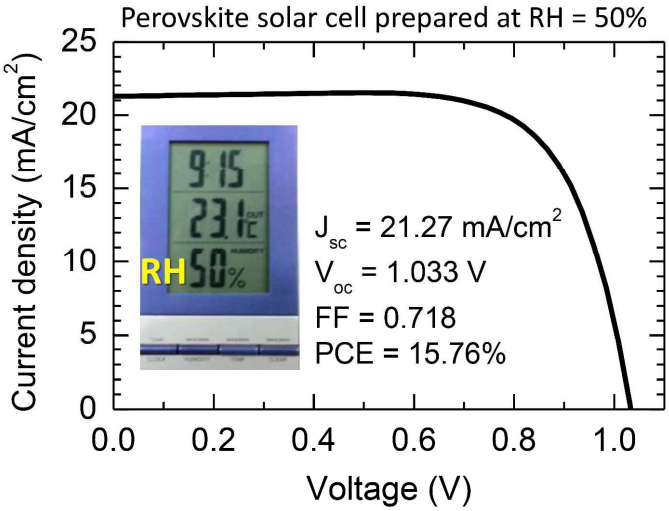

Abstract

We report here an efficient method for preparing high efficiency $CH_3NH_3PbI_3$ perovskite solar cell under high relative humidity, where morphology of PbI_2 was found to be of crucial importance. $CH_3NH_3PbI_3$ was formed on mesoporous TiO_2 layer by two-step spin coating method. During the first-step spin-coating procedure to form PbI_2 layer, FTO glass substrate was pre-heated at temperature ranging from room temperature (without pre-heating) to 60^{o}C. An average power conversion efficiency (PCE) showed 11.16 % without pre-heating, which was improved to 15.31% as the temperature of substrate (T_{sub}) was raised to 50 ^{o}C. Pre-heated substrate led to higher photocurrent and voltage than non-pre-heated one. When T_{sub} increased to 60 ^{o}C, a PCE was declined to 10.49% due to large portion of unreacted PbI_2. Compared to the non-pre-heated substrate, unreacted PbI_2 was presented on the pre-heated substrates after the second-step spin-coating of CH_3NH_3I as confirmed by X-ray diffraction and time-of-flight secondary ion mass spectroscopy (TOF-SIMS) depth profile analyses. Improved crystallinity of PbI_2 induced by substrate pre-heating was responsible for incomplete conversion of PbI_2 to $CH_3NH_3PbI_3$. Nevertheless, increases in photocurrent and voltage by pre-heating was attributed to better pore filling and surface coverage of perovskite layer, as observed by focused ion beam assisted scanning electron microscopy (FIB-SEM) images, which was associated with morphology of PbI_2 layer. According to the study on effect of $CH_3NH_3PbI_3$ thickness controlled by concentration of PbI_2, substrate temperature was found to play predominant role in determining photovoltaic performance rather than thickness. A best PCE of 15.76% was achieved along with photocurrent density of 21.27 mA/cm^2, voltage of 1.033 V and fill factor of 0.718 from the perovskite solar cell prepared in 50% relative humidity.

Keywords: Perovskite, $CH_3NH_3PbI_3$, Relative humidity, PbI_2 morphology, Substrate temperature

Introduction

Since the first report on long-term durable solid state perovskite solar cell in 2012 [1] following the reports on organo lead halides as sensitizer in liquid electrolyte based solar cell in 2009 [2] and 2011 [3], enormous attention has been focused on perovskite solar cell due to high power conversion efficiency (PCE) attained by low-cost and facile fabrication process. As a result, a PCE of 20.1% was cerfified in 2014 [4]. Solution-processed and vapor deposition methods have been proposed to achieve high quality perovskite layer and thereby high efficiency. Deposition from $PbCl_2$ and CH_3NH_3I vapors led to $CH_3NH_3PbI_3$ ($MAPbI_3$) phase with pereferred orientation and flat surafce morphology [5], which demonstrated a PCE of 15.4%. One-step spin coating using $PbCl_2$ and CH_3NH_3I could also result in highly oriented $MAPbI_3$ phase, leading to a PCE of 19.3% [6]. Solvent-enginnering thehniques were developed in one-step spin coating of PbI_2 and CH_3NH_3I, which produced large crystal domains with flat surface of $MAPbI_3$ [7,8]. One-step solvent engineering method gave recently rise to a PCE approaching 20% [9]. Apart from one-step solution process, a two-step sequential depsoition has alternatively been proposed, in which reaction of CH_3NH_3I with the spin-coated PbI_2 layer readily formed $MAPbI_3$ [10]. Crystal size was found to be controlled by varying CH_3NH_3I concentration in two-step deposition procedure and a PCE of 17.01% was achieved from large $MAPbI_3$ cuboids [11]. Regardless of preparation methods, $MAPbI_3$ has been prepared under negligable or extremely low humidity in glove box. However, preparation in the glove box may be limited to mass production from the indusrtial piont of view. We have been thus motivated to fabricate perovskite solar cell in ambient condition even under high hunidity condition. To achieve high photovoltaic performance of perovskite solar cell prepared under relative hunidity higher than >30%, modified two-step coating

method has been desgined and carfully conducted. While we were investigating and developing fabrication of high efficiency perovskite solar cell under high relative humidity condition, a method for 12.73% perovskite solar cell prepared under high relative humidity was reported using a low-pressure chemical vapor deposition technology [12].

Here we report an effective way for preparing high efficiency $MAPbI_3$ perovskite solar cell under high relative humidity. In two-step coating procedure, morphology of the PbI_2 layer deposited on the mesoporous TiO_2 coated FTO glass substrate is crucial in determining the final morphology of $MAPbI_3$ and photovoltaic performance, which is found to depend significantly on the substrate temperature while preparing the PbI_2 layer under indoor humidity. Dependence of photovoltaic performance on the substrate pre-heating temperature has been investigated. Perovskite solar cell prepared under relative humidity of around 50% demonstrated a PCE of 15.76%.

Methods

Materials synthesis. CH_3NH_3I was synthesized by reaction of 27.8 mL of CH_3NH_2 (40 wt.% in methanol, TCI) with 30 mL of HI (57 wt.% in water, Aldrich) in a round bottomed flask under vigorous stirring for 2 h in ice bath [1,3]. The precipitated CH_3NH_3I was collected using rotary evaporator at 50 ^oC for 1 h, washed with diethyl ether several times and finally dried in vacuum for 24 h. TiO_2 nanoparticles with average diameter of about 50 nm were synthesized hydrothermally according to the method reported elsewhere [13]. The seed particles with diameter of about 20 nm were first synthesized using titanium isopropoxide (97%, Aldrich) in acidic condition at 230 ^oC for 12 h. Hydrothermal procedure

was repeated to grow the seed particles. A TiO_2 paste was prepared by mixing nanocrystalline TiO_2, terpineol, ethyl cellulose and lauric acid with nominal ratio of 1.25 : 6 : 0.9 : 0.1. For controlling thickness of mesoporous TiO_2 film, the paste was further diluted with ethanol (99.9%, Samchun).

Solar cell fabrication. Solar cells were fabricated under indoor humidity, usually higher than 40%. FTO glass (Pilkington, TEC-8, 8 ohms/sq) was cleaned in a UV-Ozone cleaner for 15 min, followed by washing with detergent solution and acetone. The substrate was further cleaned by sonication in an ethanol. 60 nm-thick compact TiO_2 was formed on the cleaned FTO glass by spin-coating the 0.15 M solution of titanium diisopropoxide bis(acetylacetonate) (75 wt% in isopropanol, Aldrich) in 1-butanol (99.8%, Aldrich) at 700 rpm for 8 s, 1000 rpm for 10 s and 2000 rpm for 40 s, which was dried at 125 ^oC for 5 min. A 150 nm-thick mesoporous TiO_2 layer was formed on the compact TiO_2 layer by spin-coating the diluted TiO_2 paste (0.14 g/ml) at 2000 rpm for 20s. After the coating, the substrate was dried at 125 ^oC for 5 min and annealed at 550 ^oC for 1 h. The mesoporous TiO_2 film was post-treated with 0.02 M aqueous $TiCl_4$ (>98%, Aldrich) solution at 70 ^oC for 10 min, followed by annealing at 500 ^oC for 30 min. PbI_2 solutions were prepared by dissolving 498 (1.0 M), 392 (0.8 M) and 290 (0.6 M) mg PbI_2 (99%, Aldrich) in 1 ml *N,N*-dimethylformamide (DMF, 99.8%, Aldrich) at 60 ^oC. 20 μl of PbI_2 solution was spin-coated on the mesoporous TiO_2 film at 7000 rpm for 20 s. The solution temperature was kept at 60 ^oC while spin-coating. Before PbI_2 coating, the substrates were pre-heated at 40 ^oC, 50 ^oC, and 60 ^oC on hot plate respectively. After the coating, the film was dried at 40 ^oC for 3 min, followed by 100 ^oC for 5 min. To convert the PbI_2 layer to $MAPbI_3$, 300 μl of 0.044 M (7 mg/ml) CH_3NH_3I dissolved in 2-propanol was spin-coated on top of the PbI_2 layer at 0 rpm

for 45 s (loading time) followed by 4000 rpm for 20 s, which was dried at 100 ^{o}C for 5 min. A spiro-MeOTAD solution was prepared by dissolving 72.3 mg of spiro-MeOTAD in 1 ml chlorobenzene, in which 28.8 µl of 4-*tert*-butyl pyridine and 17.5 µl of lithium bis(trifluoromethanesulfonyl)imide (LiTFSI) solution (520 mg/1 ml acetonitrile (99.8%, Aldrich)) was added. The spiro-MeOTAD solution was spin-coated on the $MAPbI_3$ film at 4000 rpm for 20 s. Finally, gold was thermally evaporated at 1Å/s.

Characterization. Photocurrent density and voltage curves were recorded using a Keithley 2400 source meter under AM 1.5G one-sun illumination (100 mW/cm^2) provided by a solar simulator (Oriel Sol 3A class AAA). A 450 W Xenon lamp (Newport 6279NS) was used as a light source. The light intensity was adjusted using a NREL-calibrated Si solar cell equipped with KG-2 filter. During the measurement the device was covered with a metal mask with aperture area of 0.10 cm^2. Morphologies were investigated using a high-resolution field emission scanning electron microscopy (HR FE-SEM, JSM-7600F, JEOL) and a focused ion beam assisted SEM (FIB-SEM, Zeiss Auriga). The crystal structure of the PbI_2 and $MAPbI_3$ formed on the mesoporous-TiO_2 film was investigated using an X-ray diffraction measurement (XRD, D8 ADVANCE, Bruker Corporation) with Cu Kα radiation at scan rate of 4 ^{o}C/min under operation condition of 40 kV and 40 mA. The absorption spectra of PbI_2 and $MAPbI_3$ films were analyzed using an UV/VIS spectrometer (Lambda 35, Perkinelmer) in the wavelength ranging from 300 to 900 nm. Photoluminescence (PL) spectra were measured by Cary Eclipse Fluorescence Spectrophotometer (Agilent Technologies), where the excited wavelength was 530 nm and detected in the wavelength ranging from 600 to 900 nm with 10 nm increment. Depth profile of the $MAPbI_3$ films were recorded using time-of-flight secondary ion mass spectrometry (TOF-SIMS, Model-TOF-SIMS 5 of ION-

TOF GmbH, Germany), where the pulsed primary ions from a 25 keV Bi^+ liquid-metal ion gun were used to pelt down the sample surface to produce secondary ions, and 1 keV O_2 source was used to sputter out the layers from the sample surface in order to investigate the depth. The sputtering was processed on 150 × 150 μm^2, whereas the analysis was done on 40 × 40 μm^2 area for all samples. The layer thickness was measured by an alpha-step IQ surface profiler (KLA Tencor).

Results and discussion

Two-step spin coating was performed outside glove box and under indoor humidity condition. In two-step spin coating procedure in the glove box, the DMF solution of PbI_2 has been normally spin-coated on the FTO glass substrate without pre-heating the substrate. However, we found that a turbid yellow PbI_2 film was formed at indoor humidity condition, which was serious as relative humidity increased. For the case of pre-heating the substrate, the deposited PbI_2 layers become more transparent. This indicates that morphology of the deposited PbI_2 film is likely to be influenced by the substrate pre-heating. **Figure 1** shows plane-view and cross-sectional SEM images of the PbI_2 films depending on the pre-heating temperature. Imperfect coverage of PbI_2 on the substrate with porous nature is observed without pre-heating, whereas the substrate is fully covered with PbI_2 when the substrate is pre-heated. It is also found that perovskite is well infiltrated in mesopores of TiO_2 film upon pre-heating the substrate compared to non-pre-heated substrate. The PbI_2 layer thickness increases with increasing the pre-heating temperature from 40 ^oC to 60 ^oC. Average thickness of the PbI_2 film is estimated to be 300 nm, 350 nm, 400 nm and 540 nm without pre-heating

and with pre-heating at 40 ^{o}C, 50 ^{o}C and 60 ^{o}C, respectively. This increase seems to be related to competition between solvent evaporation rate and PbI_2 crystallization rate, that is, PbI_2 crystallization rate becomes higher than the solvent evaporation rate as the pre-heating temperature increases.

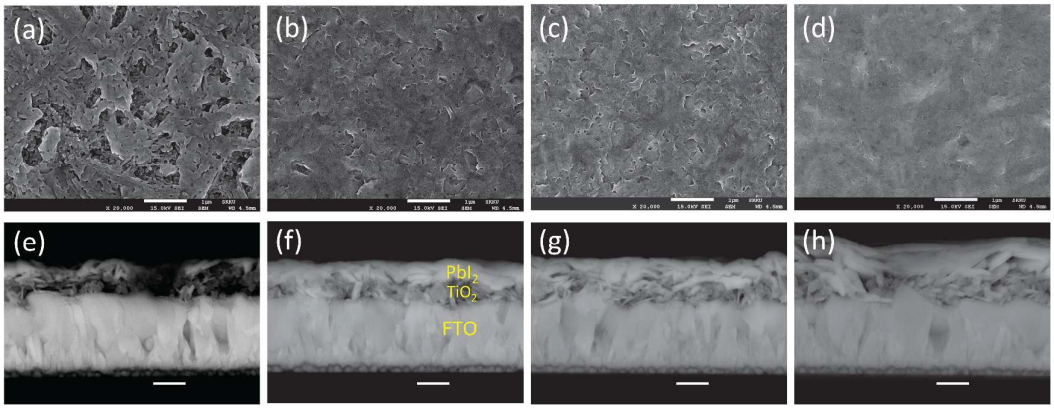

Fig. 1 Plane-view SEM images of PbI_2 layer deposited on the mesoporous TiO_2 coated FTO substrate, where the substrate was preheated at (a) room temperature (without pre-heating), (b) 40 ^{o}C, (c) 50 ^{o}C and (d) 60 ^{o}C and (e-h) corresponding cross-sectional SEM images. Scale bars in (a-d) represent 1 um and 300 nm in (e-h).

Figure 2 shows SEM images of $MAPbI_3$ formed by spin-coating of CH_3NH_3I solution on the PbI_2 coated substrate prepared at different substrate temperature. Cuboid $MAPbI_3$ crystals formed with gaps between crystals while depositing CH_3NH_3I on the PbI_2 prepared without pre-heating (Figure 2(a)). On the other hand, cuboids are closely packed when the substrates are pre-heated (Figures 2(b)-(d)). It is noted that $MAPbI_3$ size is bigger as the pre-heating temperature increase (~ 200 nm without pre-heating, ~400 nm at 40 ^{o}C and 50 ^{o}C and ~800 nm at 60 ^{o}C), which is associated with conversion rate of PbI_2 to $MAPbI_3$. If the conversion reaction requires longer time, crystal is expected to grow bigger. It was reported that it took very long time (several days) to get large sized single crystal $MAPbI_3$ [14-17],

which means that slow reaction leads to large crystal. Thus, an increase in $MAPbI_3$ crystal with pre-heating temperature is probably ascribed to slower reaction due to the increased crystallinity and in part thickness of PbI_2.

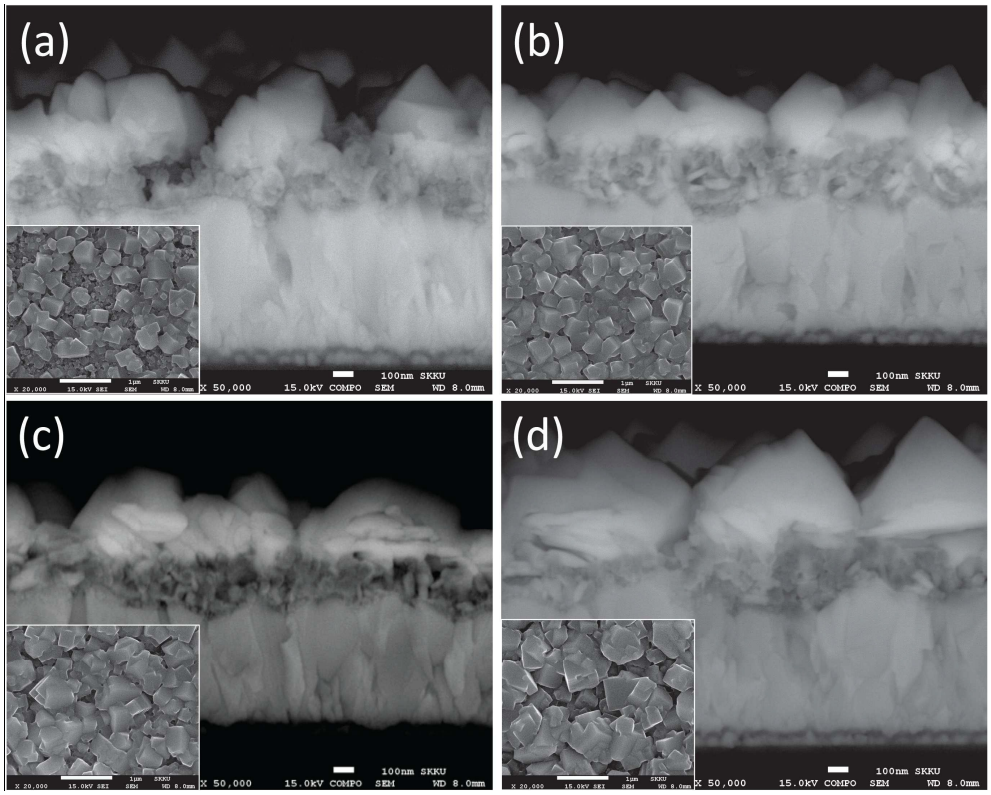

Fig. 2 Cross-sectional and plane-view (insets) SEM images of $CH_3NH_3PbI_3$ ($MAPbI_3$) formed by deposition of CH_3NH_3I on the PbI_2 layer formed at substrate temperature of (a) room temperature (without pre-heating), (b) 40 ^oC, (c) 50 ^oC and (d) 60 ^oC. Scale bars represent 100 nm (1 μm in insets).

X-ray diffraction was performed to investigate any change in crystallinity depending on the substrate pre-heating temperature. **Figure 3(a)** shows XRD patterns of the PbI_2 films on the mesoporous TiO_2 coated FTO glass at different pre-heating temperature. The (001) peak at 2 theta = 12.6^o becomes intense and its full width at half maximum (FWHM) is narrowed after pre-heating and as the pre-heating temperature increases, which indicates that

crystallinity and X-ray crystallite size increase simultaneously. Such an improved crystallinity of PbI_2 is expected to retard the conversion of PbI_2 into $MAPbI_3$. **Figure 3(b)** shows XRD patterns of $MAPbI_3$. Compared to full conversion of PbI_2 into $MAPbI_3$ without pre-heating, unreacted PbI_2 peak appears upon pre-heating the substrate and its intensity increases as the pre-heating temperature increase. As expected, large portion of the unreacted PbI_2 at high substrate pre-heating temperature is attributed to the improved crystallinity of the deposited PbI_2, associated with longer reaction period. We have tried to convert fully the PbI_2 prepared at pre-heating temperature of 60 ^oC into $MAPbI_3$ by prolonged the loading time of CH_3NH_3I, it was however hard to be successful because PbI_2 would start to dissolve partially at long exposure to 2-propanol. Although some unreacted PbI_2 is presented in the film, the residual PbI_2 was reported to bring about a passivation effect in perovskite solar cells [18].

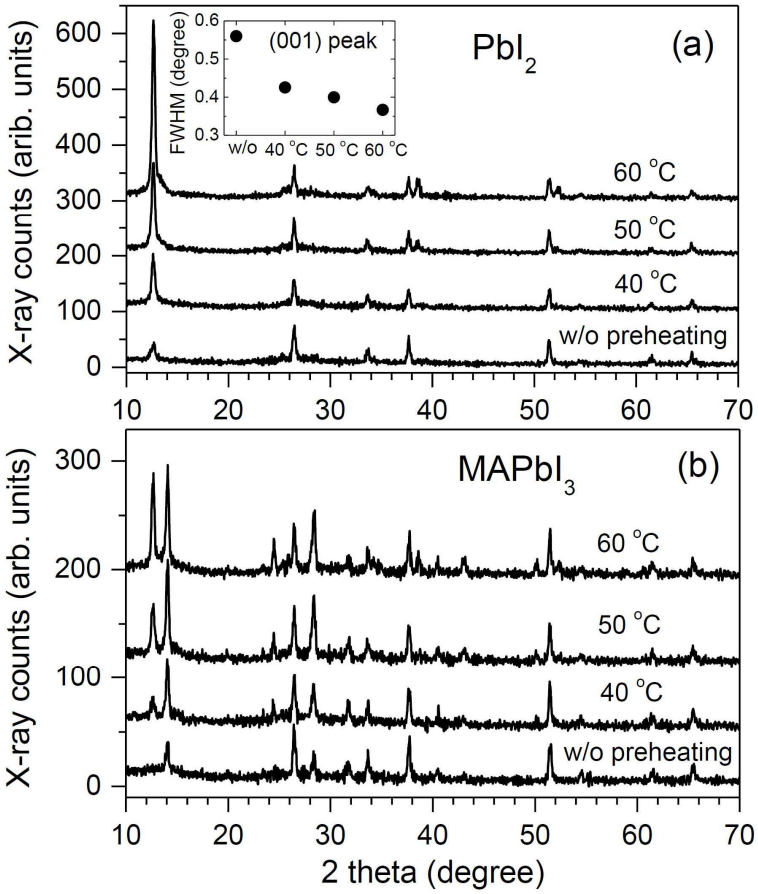

Fig. 3 X-ray diffraction patterns of (a) PbI_2 and (b) $MAPbI_3$ films depending on the substrate temperature. Inset in (a) shows full width at half maximum (FWHM) of (001) peak of PbI_2. The data were collected using PbI_2 and $MAPbI_3$ film formed on mesoporous TiO_2 deposited FTO glass substrates.

TOF-SIMS depth profiling was carried out for elemental analysis in the film. **Figure 4** displays the depth profile of the $MAPbI_3$ layer formed on the mesoporous TiO_2 coated FTO glass substrate depending on the substrate pre-heating temperature. Elements of C, N, H, Pb, I, Ti, O, Sn and F were detected, where H, N, Pb, I, Ti, O and Sn are displayed in the figure. As can be seen in **Figure 4**, Pb decreases in parallel with I and then their intensities are not changed with time. Large cuboid of perovskite results in inhomogeneous perovskite capping

layer, and both parts with thin and thick perovskite capping layer are etched simultaneously during the TOF-SIMS measurement. As a result, the Pb and I profiles appear to decrease when crossing the perovskite capping layer. This indicates that Pb and I are in the same compound such as $MAPbI_3$ and/or PbI_2. Ti and O increase simultaneously and then their intensities are saturated, which is due to mesoporous TiO_2 film. For the case of without pre-heating the substrate, the intensities of Pb and I decrease gradually upto about 100 s (Figure 4(a)), while those decreases upto 180 s for the case of 60 ^oC-pre-heated case (Figure 4(d)). This indicates that the latter case has thicker $MAPbI_3$ layer. Since no PbI_2 peak is detected for the non-pre-heated case, depth profiling of Pb and I comes from pure $MAPbI_3$. There is difference in depth profile when comparing depth profile of Pb and I for the 60 ^oC-pre-heated sample with that for the non-pre-heated one in Figure 4(a) and (d), which may be due to the presence of PbI_2 as detected by XRD. Pb content in PbI_2 is 50% with respect to iodide, while Pb is 33% in $MAPbI_3$. The decreasing rate of Pb from 0 s to 100 s in the 60 ^oC-pre-heated sample is slower than that in the non-pre-heated one, which is indicative of higher Pb content. The unreacted PbI_2 is probably to be presented in bulk of perovskite capping layer, because the conversion of PbI_2 in bulk of thin film into $MAPbI_3$ takes much longer time compared to the conversion rate of PbI_2 in the pores of mesoporous TiO_2 film. It has been reported that CH_3NH_3I insertion hardly proceeds beyond the surface of thin PbI_2 films, and that the complete transformation of the crystal structure requires several hours while the conversion of PbI_2 in mesoporous TiO_2 into $MAPbI_3$ is completed within one minute [10]. If the wide band gap insulating PbI_2 layer is presented near the FTO, charge collection at FTO may be significantly hindered by the unreacted PbI_2 layer. However, all the samples prepared by pre-heating the substrate shows higher photocurrent despite the presence of PbI_2 (see Figure 5), supporting the unreacted PbI_2 exists in the bulk of $MAPbI_3$ capping layer.

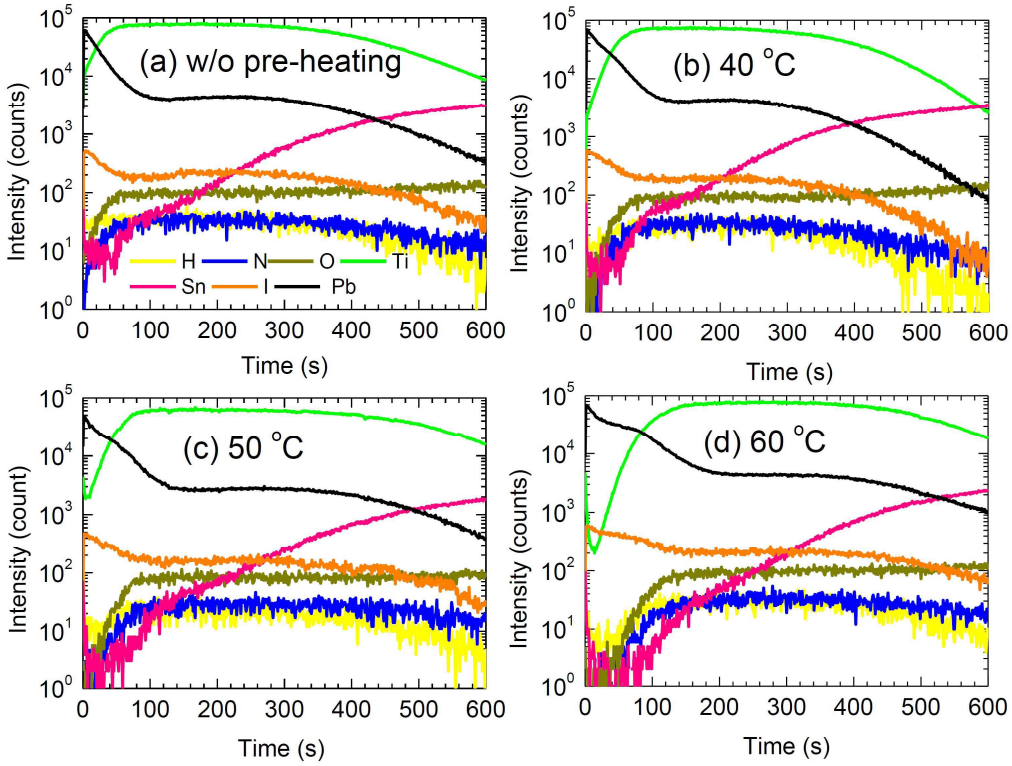

Fig. 4. Time-of-flight secondary ion mass spectroscopy (TOF-SIMS) profile for the $MAPbI_3$ layer formed on the mesoporous TiO_2 deposited FTO glass substrate by reacting CH_3NH_3I with the PbI_2 deposited at substrate temperature of (a) without pre-heating, (b) 40 °C, (c) 50 °C and (d) 60 °C. Depth profiling was performed from perovskite layer to FTO substrate.

Figure 5 shows short-circuit photocurrent density (J_{sc}), open-circuit voltage (V_{oc}), fill factor (FF) and power conversion efficiency (PCE) depending on the pre-heating temperature. The average photovoltaic parameters are listed in **Table 1**. J_{sc} and V_{oc} are significantly higher for the 40 °C- and 50 °C-pre-heated cases than for the non-pre-heated one. In addition, FF is slightly higher for the pre-heated cases. J_{sc} is improved from 16.94 mA/cm^2 for the non-pre-heated case to 19.63 and to 20.71 mA/cm^2 upon deposition of PbI_2 on the 40 °C- and 50 °C-pre-heated substrates, respectively. V_{oc} is also enhanced from 937 mV to 1012 and 1017 mV. As a result, average PCE is improved from 11.16% to 14.53 and 15.31%. On the other hand,

the device prepared based on 60 ^{o}C-pre-heating procedure deteriorates PCE to 10.49% along with large standard deviation. Compared to the non-pre-heated case, the lower PCE of the 60 ^{o}C-pre-heated case is mainly due to lower FF in spite of slightly higher J_{sc} and V_{oc}. The superior performance obtained by pre-heating procedure (40 ^{o}C and 50 ^{o}C) is due to morphology of $MAPbI_3$ determined by the deposited PbI_2 morphology, as investigated previously. To understand property-structure relation, FIB-assisted SEM images are obtained for the full cell.

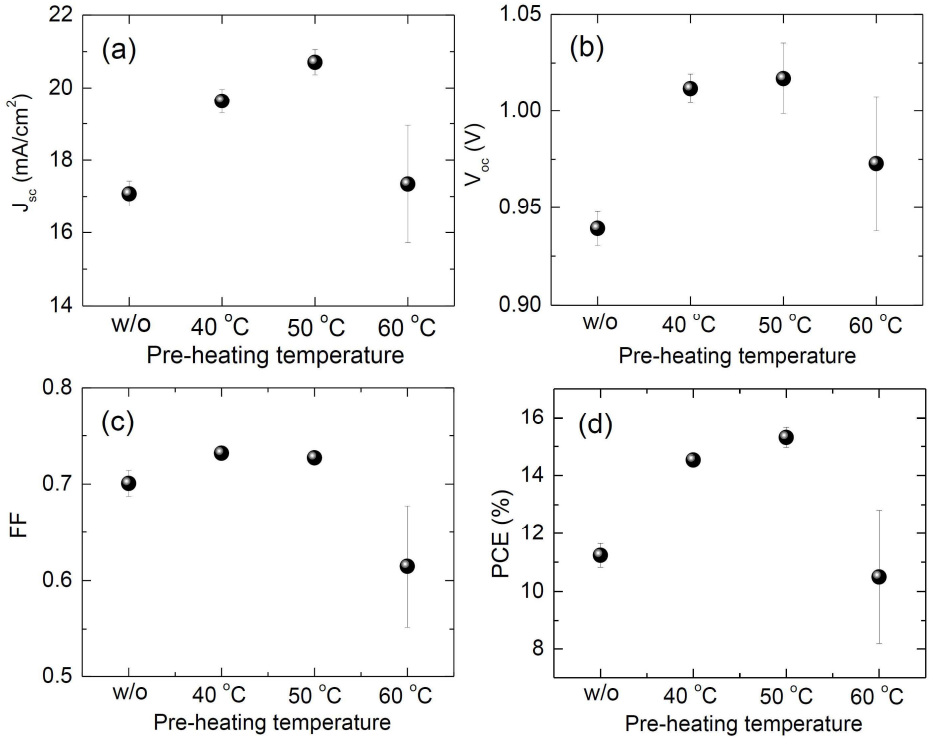

Fig. 5 Effect of substrate pre-heating temperature on (a) short-circuit photocurrent density (J_{sc}), (b) open-circuit voltage (V_{oc}), (c) fill factor (FF) and (d) power conversion efficiency (PCE).

Table 1. Short-circuit current density (J_{sc}), open-circuit voltage (V_{oc}), fill factor (FF) and power conversion efficiency (PCE) of $MAPbI_3$ solar cells by pre-heating conditions at AM 1.5G one-sun illumination (100 mW/cm^2). Relative humidity was about 44%.

Pre-heating temperature	J_{sc} (mA/cm^2)	V_{oc} (V)	FF	PCE (%)
w/o	16.94±0.47	0.937±0.010	0.70±0.01	11.16±0.43
40 ^{o}C	19.63±0.33	1.012±0.007	0.73±0.01	14.53±0.17
50 ^{o}C	20.71±0.35	1.017±0.018	0.73±0.01	15.31±0.35
60 ^{o}C	17.34±1.62	0.970±0.030	0.61±0.06	10.49±2.31

FIB-SEM images for the full cell in **Figure 6** shows clearly each layer. The mesoporous TiO_2 film is not fully covered by the $MAPbI_3$ crystals when processing without pre-heating as can be seen in Figure 6(a). The uncovered TiO_2 is directly contacted with spiro-MeOTAD, which is likely to be responsible for low V_{oc} due to recombination [19]. The relatively low J_{sc} may be attributed to low $MAPbI_3$ coverage. The coverage of the TiO_2 layer with $MAPbI_3$ becomes better by substrate pre-heating and fully covered upon pre-heating the substrate at 50 ^{o}C (Figure 6(c)). Thus higher V_{oc} along with higher J_{sc} can be explained by morphology and coverage of $MAPbI_3$ for 40 ^{o}C- and 50 ^{o}C-pre-heating cases. It is noted that large $MAPbI_3$ crystals does not fully cover the TiO_2 film upon pre-heating at 60 ^{o}C (Figure 6(d)), which deteriorates J_{sc} and V_{oc} being close to those obtained without pre-heating. Moreover the increased capping layer thickness of $MAPbI_3$ for 60 ^{o}C-pre-heating is in part responsible for low FF due to increase in resistance [20,21]. From the cross-sectional SEM study on full cell structure, the highest performance obtained by the 50 ^{o}C-pre-heating procedure can be explained.

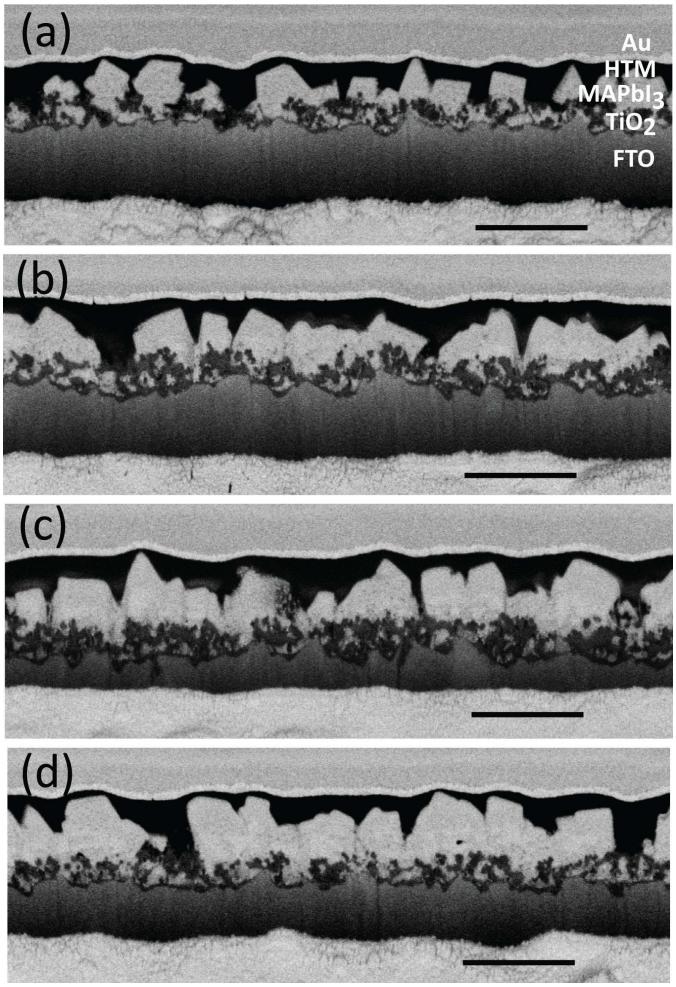

Fig. 6 Focused ion beam (FIB) assisted SEM images of full cells with $MAPbI_3$ perovskite layer formed by reacting CH_3NH_3I with the PbI_2 layer deposited at substrate temperature of (a) without pre-heating, (b) 40 ^oC, (c) 50 ^oC and (d) 60 ^oC. Scale bars represent 1 μm.

Figure 7 compares PL intensity of $MAPbI_3$ film depending on the pre-heating temperature. The sample for PL measurement is composed of $MAPbI_3$ film deposited on mesoporous TiO_2 coated FTO substrate (see the inset in Figure 7). The emission peaks appeared in 750 nm – 800 nm range are resulted from PL of $MAPbI_3$ because the emissive photon energy is corresponding to band gap of about 1.6 eV [22]. The PL peaks shift to longer wavelength as the pre-heating temperature increases. Since PL of perovskites is

expected to occur due to recombination of localized excitons, the bathochromic shift of both absorption (not shown here) and PL spectra can be attributed to less localized exciton states in large crystals. In addition, compared to the non-pre-heating case, the PL intensity decreases significantly upon pre-heating. When considering higher coverage of $MAPbI_3$ for the pre-heated cases than the non-preheated one, the reduced PL intensity is due to better electron injection into mesoprous TiO_2. This is well consistent with interfacial morphology as confirmed by FIB-SEM. The improved J_{sc} is related to better charge separation and thereby charge collection. The lowest PL intensity observed for the 60 ^{o}C-pre-heating case is indicative of more effective charge separation occurred at TiO_2/perovskite interface. However, despite such an effective charge separation, the increased capping layer thickness and partially uncovered TiO_2 film are responsible for low J_{sc} and V_{oc}.

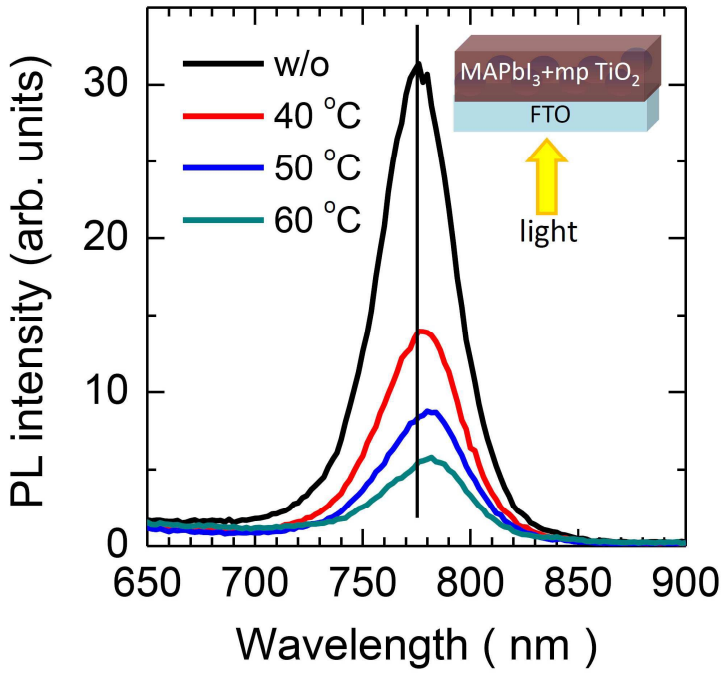

Fig. 7 Photoluminescence (PL) spectra of the $MAPbI_3$ layers deposited on FTO substrate showing effect of substrate temperature. Inset shows incident light on FTO side.

We investigated effect of preparation condition on I-V hysteresis. **Figure 8** compares I-V hysteresis, where no significant I-V hysteresis in terms of scan direction is observed for the device prepared without pre-heating condition. On the other hand, I-V hysteresis is pronounced as pre-heating temperature increase and serious at 60 ^{o}C-pre-heating condition. It was reported that I-V hysteresis was dependent on $MAPbI_3$ crystal size and presence and absence of mesoporous TiO_2 layer [23], where serious I-V hysteresis was observed from planar structure (without mesoporous TiO_2 layer) and smaller crystal. Compared to the less I-V hysteresis from the non-pre-heating condition, the pronounced I-V hysteresis for the pre-heating condition is due to the increased capping layer at the same thickness of TiO_2.

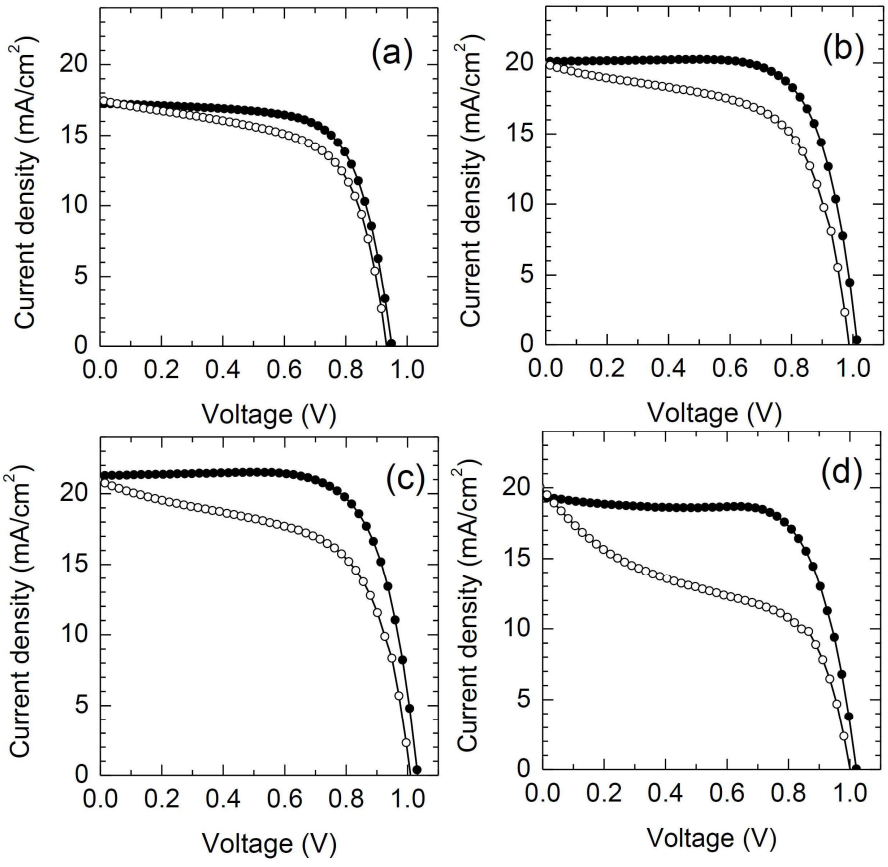

Fig. 8 J-V curves depending on reverse scan (filled circles) and forward scan (empty circles) for the device with $MAPbI_3$ prepared by reaction of CH_3NH_3I with the PbI_2 layer deposited at substrate temperature of (a) without pre-heating, (b) 40 ^oC, (c) 50 ^oC and (d) 60 ^oC. J-V measurements were performed under AM 1.5G one sun illumination.

Since the thickness and crystallinity of PbI_2 and $MAPbI_3$ could be changed by not only substrate temperature but also concentration of PbI_2, it is required to investigate effect of concentration of PbI_2 (1.0, 0.8 and 0.6 M) on photovoltaic performance at different substrate temperature (50 ^oC and 60 ^oC). **Figure 9** shows J-V curves, XRD and SEM images depending on the PbI_2 concentration at 50 ^oC and 60 ^oC. Photovoltaic parameters along with PbI_2 and $MAPbI_3$ film thickness are summarized in **Table 2**. As expected, the thickness of $MAPbI_3$ decreases with increasing the concentration of PbI_2 solution from 1.0 M to 0.6 M. On the other hand, the $MAPbI_3$ thickness increases as the substrate temperature increases from 50 ^oC to 60 ^oC. It is noted that J_{sc}, V_{oc} and FF decrease simultaneously as the concentration of PbI_2 decreases regardless of the substrate temperature. Consequently PCEs decrease from 15.01% to 11.03% at 50 ^oC and from 14.53% to 11.24% at 60 ^oC. In addition, when comparing the photovoltaic performance for the similar $MAPbI_3$ thickness (~665 nm for the 1.0 M PbI_2 at 50 ^oC and ~602 nm for the 0.8 M at 60 ^oC), the device prepared at 50 ^oC with 1.0 M PbI_2 shows better photovoltaic performance. This indicates that substrate temperature plays more important role in determining the performance rather than film thickness. The basis for the difference in the performance is due to the fact that higher amount of unreacted PbI_2 originated from higher crystallinity of PbI_2 at higher temperature, as confirmed by XRD in **Figures 9(c) and (d)**, leads to lower J_{sc} and FF. The lower V_{oc} at higher substrate temperature is probably due to direct contact of hole transporting layer with mesoporous TiO_2 as can be seen in **Figure 9 (f)**, which might result from larger cuboid formed by higher crystallinity of

PbI_2. For the case of devices prepared at 60 °C, the photovoltaic performance was found to be sensitive to humidity compared to other temperatures. PCE was reproducibly observed to be relatively low at high humidity (see Table 1) but improved at low humidity (Table 2). We can draw conclusion that the photovoltaic performance of perovskite solar cell prepared at ambient environment is mainly influenced by substrate temperature.

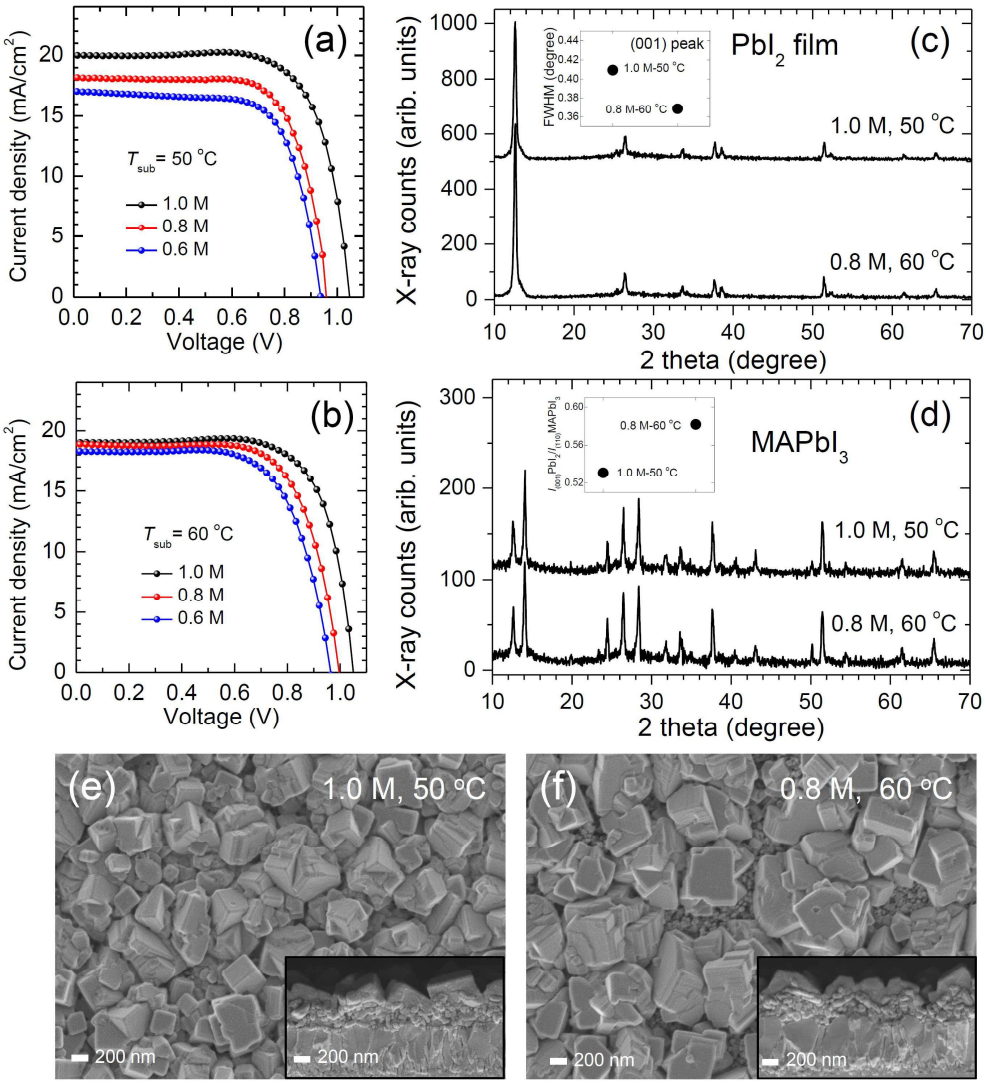

Fig. 9 J-V curves of perovskite solar cells as a function of the concentration of PbI_2 solution (1.0, 0.8 and 0.6 M) at substrate temperature (T_{sub}) of (a) 50 °C and (b) 60 °C, measured at

AM 1.5 G one sun illumination. XRD patterns of (c) PbI_2 and (d) $MAPbI_3$ films formed from 1.0 M-50 ^oC and 0.8 M-60 ^oC conditions, where insets show FWHM of (001) peak for PbI_2 and peak intensity ratio of (001) peak of PbI_2 to (110) peak of $MAPbI_3$. SEM images of $MAPbI_3$ formed from (e) 1.0 M-50 ^oC and (f) 0.8M-60 ^oC conditions, where insets show cross-sectional images. The J-V data and SEM images shown here were obtained from the devices prepared at relative humidity of less than 20%.

Table 2. Photovoltaic parameters and thicknesses depending on the PbI_2 concentration and substrate temperature. Photovoltaic parameters were measured at AM 1.5 G one sun illumination. Average values were obtained from 9 cells. Relative humidity was <20%.

T_{sub} (^oC)	[PbI_2] (M)	Thickness (nm) PbI_2($MAPbI_3$)	J_{sc} (mA/cm^2)	V_{oc} (V)	FF	PCE (%)
50 ^oC	1.0	414.2 (665.6)	19.84±0.30	1.042±0.004	0.73±0.01	15.01±0.35
	0.8	252.7 (513.6)	18.32±0.83	0.953±0.013	0.71±0.01	12.36±0.54
	0.6	231.5 (510.2)	17.11±0.70	0.935±0.013	0.69±0.01	11.03±0.46
60 ^oC	1.0	545.2 (742.6)	19.09±0.29	1.051±0.009	0.72±0.01	14.53±0.32
	0.8	461.8 (602.3)	18.90±0.37	0.986±0.022	0.70±0.01	12.97±0.43
	0.6	311.1 (459.3)	18.25±0.61	0.926±0.027	0.66±0.03	11.24±0.97

The best performing device with a PCE of 15.76% is obtained by two-step deposition procedure based on the 50 ^oC-pre-heating condition under relative humidity of 50% (**Figure 10**). Under high relative humidity condition, the procedure of pre-heating the substrate for the PbI_2 deposition is crucial and important to achieve high efficiency because the PbI_2 deposition process is sensitive to humidity.

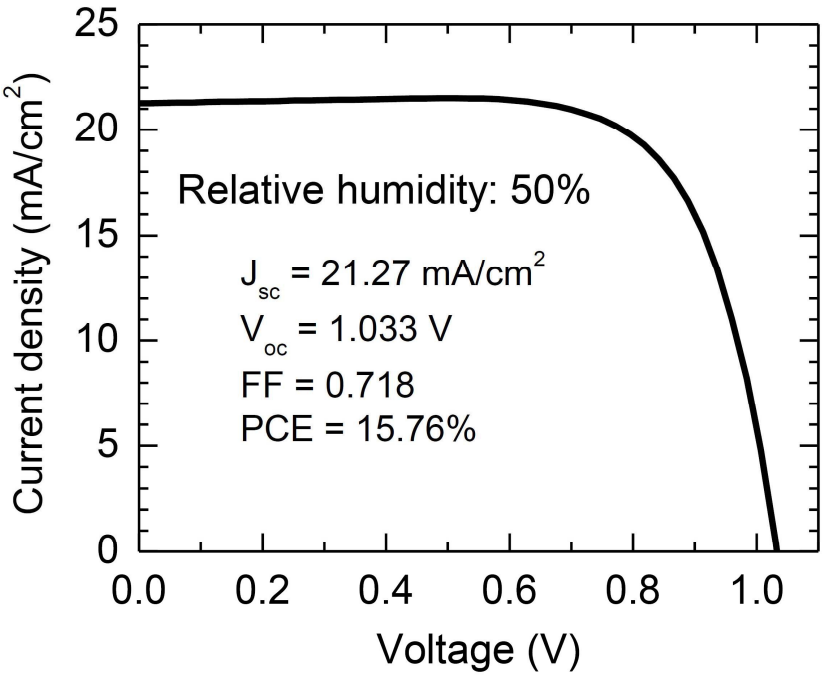

Fig. 10 J-V curve of the best performing perovskite solar cell prepared in the relative humidity of 50%. $MAPbI_3$ was formed by reacting CH_3NH_3I with the PbI_2 layer deposited at substrate temperature of 50 ^oC. Data was collected by reverse scan at AM 1.5 G one sun illumination.

Conclusions

We developed an effective way to fabricate perovskite solar cell with high photovoltaic performance exceeding 15% under high relative humidity condition, in which the substrate pre-heating process for PbI_2 deposition in two-step coating procedure was important. While spin-coating of the PbI_2 solution, the pre-heated substrate led to infiltration of PbI_2 in the mesopores of TiO_2 film full coverage of the TiO_2 film with PbI_2. Optimal pre-heating temperature was around 50 ^oC at least in our experimental procedure. We also tried to investigate effect of pre-heating on photovoltaic performance for the one-step deposition condition, where preliminary results showed that pre-heating method did not work well for

one-step deposition under high relative humidity, more than 40%. This indicates that the PbI_2 coting process is most critical in producing high quality $MAPbI_3$ under high relative humidity condition. Without pre-heating condition, average PCE of 10-11% is observed, while PCE over 15% is reproducibly achieved by the substrate pre-heating process.

Acknowledgement

This work was supported by the National Research Foundation of Korea (NRF) grants funded by the Ministry of Science, ICT & Future Planning (MSIP) of Korea under contracts No. NRF-2010-0014992, NRF-2009-0092951, NRF-2012M3A6A7054861 (Global Frontier R&D Program on Center for Multiscale Energy System). We thank S. M. Kang and N. Y. Ahn for FIB-SEM measurement.

Reference

1. H.-S. Kim, C.-R. Lee, J.-H. Im, K.-B. Lee, T. Moehl, A. Marchioro, S.-J. Moon, R. Humphry-Baker, J.-H. Yum, J. E. Moser, M. Grätzel and N.-G. Park, *Sci. Rep.*, 2012, **2**, 591.

2. A. Kojima, K. Teshima, Y. Shirai and T. Miyasaka, *J. Am. Chem. Soc.*, 2009, **131**, 6050-6051.

3. J.-H. Im, C.-R. Lee, J.-W. Lee, S.-W. Park and N.-G. Park, *Nanoscale*, 2011, **3**, 4088-4093.

4. http://www.nrel.gov/ncpv/images/efficiency_chart.jpg

5. M. Liu, M. B. Johnston and H. J. Snaith, *Nature*, 2013, **501**, 395-398.

6. H. P. Zhou, Q. Chen, G. Li, S. Luo, T. B. Song, H. S. Duan, Z. R. Hong, J. B. You, Y. S. Liu and Y. Yang, *Science*, 2014, **345**, 542-546.

7. N. J. Jeon, J. H. Noh, Y. C. Kim, W. S. Yang, S. Ryu and S. I. Seok, *Nat.Mater*., 2014, **13**, 897-903.

8. M. Xiao, F. Huang, W. Huang,Y. Dkhissi, Y. Zhu, J. Etheridge, A. Gray-Weale, U. Bach, Y.-B. Cheng, and L. Spiccia, *Angew*. *Chem*. 2014, **126**, 10056-10061.

9. N. J. Jeon, J. H. Noh, W. S. Yang, Y. C. Kim, S. Ryu, J. Seo and S. I. Seok, *Nature,* 2015, doi:10.1038/nature14133.

10. J. Burschka, N. Pellet, S.-J. Moon, R. Humphry-Baker, P. Gao1, M. K. Nazeeruddin and M. Grätzel, *Nature,* 2013, **499**, 316-319.

11. J.-H. Im, I.-H. Jang, N. Pellet, M. Grätzel and N.-G. Park, *Nature Nanotech*., 2014, **9**, 927-932.

12. P. Luo, Z. Liu, W. Xia, C. Yuan, J. Cheng and Y. Lu, *ACS Appl. Mater. Interfaces*, DOI: 10.1021/am5077588 (Web published Jan. 12, 2015)

13. J.-W. Lee, T.-Y. Lee, P. J. Yoo, M. Grätzel, S. Mhaisalkar and N.-G. Park, *J. Mater. Chem. A*, 2014, **2**, 9251-9259.

14. C. C. Stoumpos, C. D. Malliakas and M. G. Kanatzidis, *Inorg*. *Chem*., 2013, **52**, 9019-9038.

15. T. Baikie, Y. Fang, J. M. Kadro, M. Schreyer, F. Wei, S. G. Mhaisalkar, M. Grätzel and T. J. White, *J. Mater*. *Chem*. *A*, 2013, **1**, 5628-5641.

16. A. Pisoni, J. Jaćimović, O. S. Barišić, M. Spina, R. Gaál, L. Forró and E. Horváth, *J. Phys*. *Chem*. *Lett*., 2014, **5**, 2488-2492.

17. Y. Dang, Y. Liu, Y. Sun, D. Yuan, X. Liu, W. Lu, G. Liu, H. Xia and X. Tao, *CrystEngComm*, 2015, **17**, 665-670.

18. Q. Chen, H. Zhou, T.-B. Song, S. Luo, Z. Hong H.-S. Duan, L. Dou, Y. Liu and Y. Yang, *Nano Lett*., 2014, **14**, 4158-4163.

19. J.-H. Im, H.-S. Kim and N.-G. Park, *APL Mater*., 2014, **2**, 081510.

20. J.-W. Lee, D.-J. Seol, A.-N. Cho and N.-G. Park, *Adv. Mater*. 2014, **26**, 4991-4998.

21. J. M. Ball, M. M. Lee, A. Hey and H. J. Snaith, *Energy Environ*. *Sci*., 2013, **6**, 1739-1743.

22. H. S. Jung and N.-G. Park, *Small*, 2014, **11**, 10-25.

23. H.-S. Kim and N.-G. Park, *J. Phys*. *Chem*. *Lett*., 2014, **5**, 2927-2934.